

Novel Design of a Model Reference Adaptive Controller for Soft Tissue Operations

József K. Tar, Levente Kovács, Árpád Takács, Bence Takács, Péter Zentay, Tamás Haidegger, Imre J. Rudas
 Antal Bejczy Center for Intelligent Robotics
 Óbuda University, Budapest, Hungary
 Email: {tar.jozsef@nik., kovacs.levente@nik., arpad.takacs@irob., bence.takacs@irob., zentay.peter@bkg., haidegger@irob., rudas@}uni-obuda.hu

Abstract—Model Reference Adaptive Controllers (MRAC) have dual functionality: besides guaranteeing precise trajectory tracking of the controlled system, they have to provide an “external control loop” with the illusion that it controls a physical system of prescribed dynamic properties, i.e., the “reference system”. The MRACs are designed traditionally by Lyapunov’s 2nd method that is mathematically complicated, requiring strong skills from the designer. Adaptive controllers alternatively designed by the use of Robust Fixed Point Transformations (RFPT) operate according to Banach’s Fixed Point Theorem, and are normally simple iterative constructions that also have a standard variant for MRAC design. This controller assumes a single actuator that is driven adaptively. Master–Slave Systems form a distinct class of practical applications, in which two arms—the master and the slave—operate simultaneously. The movement of the master must be tracked precisely by the slave in spite of the quite different forces exerted by them. In the present paper, a soft tissue-cutting operation by a master–slave structure is simulated. The master arm has a simple torque–reference friction model, and is driven by the surgeon. The obtained master arm trajectory has to be precisely tracked by the electric DC motor driven slave system, which is in dynamic interaction with the actual tissue under operation. It is shown via simulations that the RFPT-based design can efficiently solve such tasks without considerable mathematical complexity.

I. INTRODUCTION

From the control engineering point of view, modeling and model-based tackling of friction remained a challenge even in our days. It has been realized in the 1970s that friction plays significant role in determining the characteristics of hydraulic devices [1]. The early attempts to model friction applied *static models* [2], [3], [4], [5]. The road–tire interaction (that plays crucial role in braking and driving vehicles) can be regarded as a particular problem class that has been addressed by significant research effort [6]. The inherent nonlinearity of these models were mathematically approximated in various manners. The “magic formula” invented in the ’90s contained highly nonlinear trigonometrical functions with parameters for the identification [7], [8], [9].

The *static modeling approach* had the inherent difficulty dealing with the slow speed (near “zero velocity”) motion and the phenomenon of *sticking*. *Dynamic friction models* evaded this problem via the introduction of an internal state variable belonging to a subsystem that is dynamically coupled to the controlled one [10], [11], [12]. For practical applications,

simpler nonlinear models were introduced that put together various mathematical approximations at connected velocity segments [13] (also applied in [14], [15]).

Arguably, the friction and sticking phenomena also play significant role in certain medical procedures in which the surgeon’s tool is in dynamic interaction with soft and wet tissue. The phenomenon of *slipping*, i.e., the fast reduction in the friction force with increasing velocity following an increasing phase may mean considerable inconvenience, even in the field of robotic surgery. It is reasonable to assume that dealing with a drag force—the monotone increasing function of the velocity—is easier than coping with the phenomenon of slipping. There is a distinct need for solving control problems related to sticking materials.

The traditional (either robust or adaptive) controllers were designed by the use of Lyapunov’s 2nd method [16], [17], [18], [19], [20]. Although it is not difficult to understand the essence of this design method, its practical application is not easy, since it demands very strong skills in mathematics. Further problem is the fact that these controllers concentrate on guaranteeing global stability and cannot reveal the details of the trajectory tracking error relaxation that may be the primary design intent in surgical operations needing precise trajectory tracking. Normally, the positive definite matrices in the Lyapunov function contain a lot of arbitrary control parameters that are not optimally set, though they significantly affect tracking error relaxation.

To evade the difficulties related to the Lyapunov function-based design (as an alternative adaptive design method) the RFPT-based design was introduced in [21]. This method realizes a special iterative control, in which the iterative sequence is obtained by contractive map in a Banach Space and it converges on the basis of Banach’s *Fixed Point Theorem* [22]. In contrast to the Lyapunov function-based design, this method concentrates on the realization of a prescribed trajectory tracking error relaxation, and in its simplest form, needs altogether only three adaptive parameters that can be fixed for the great majority of the applications. The weak point of this method is that it can guarantee only a bounded basin of convergence that may be left by the system. If necessary (e.g., for maintaining the convergence), one of its parameters can be adaptively tuned by various manners [23], [24], [25]. This design has the advantage that it does not need any precise model of

the system to be controlled. It can work with a preliminary approximate model: without trying to amend this model, it adaptively deforms its input via observing the behavior of the controlled system. Since no model improvement happens during this control, it always needs fresh observations and cannot promise asymptotic stability due to the principle of causality.

The above mentioned general difficulties exist for the particular class of the Lyapunov function-based adaptive controllers, the MRAC controllers (e.g., [26], [27], [28], [29]) that have double functionalities: besides guaranteeing precise trajectory tracking of the controlled system, they have to provide an “external control loop” with the illusion that it controls a physical system of prescribed dynamic properties, i.e., the reference system. Fortunately, it is straightforward to develop a particular RFPT-based design for the MRAC controllers [30] that was invented for a single driven arm. However, the use of MRAC controllers in robotized surgical operations seems to be a promising and reasonable idea since in a master–slave construction it can provide the surgeon in the role of the “external control loop”. This leads to the impression that he/she works with a well-behaving material that is exempt of the phenomenon of slipping. It is entirely the robot’s task to properly tackle this phenomenon.

The aim of this paper is to publish the results of preliminary in silico investigations on the possible realization of a master–slave type MRAC controller for surgical operations that works on the basis of the RFPT-based design. The design consists of the following key components:

- the *nominal trajectory*: must be traced by the surgical tool independently of the actual forces needed for the operation,
- the *surgeon as a controller*: trying to realize the nominal trajectory with the feeling that he/she works with the well-behaving reference system (in this way, it is guaranteed that the details of the realized motion is determined by the human instead of the machine),
- the slave robot that precisely follows the trajectory determined by the motion of the doctor’s hand while dealing with the actual dynamic properties of the tissue under operation.

Accordingly, the paper is constructed as follows: at first, the *nominal motion–reference material–surgeon* triplet is modeled as the master system. Following that, the electric DC motor driven tool, i.e., the slave system’s model and its order reduced adaptive control is described. Next, simulation results are presented and discussed, and finally the conclusions are drawn.

II. THE MODEL OF THE MASTER SYSTEM

It is assumed that there is a master arm directly operated by the surgeon who wishes to track a nominal trajectory $q^N(t)$, forged from e.g., motion primitives constructed based on a pre-operative plan. The surgical tool is assumed to be connected to this rotary axle via a gear ratio $\nu = 0.1$ and an arm of length $S = 0.05 m$. Assume that the hand of the surgeon can

be modeled as a controller who tries to realize a kinematically prescribed PD-type trajectory tracking policy as follows:

$$\ddot{q}^{MDes} = \left(\frac{d}{dt} + \Lambda_M\right)^2 (q^N - q^M) = 0 \implies \ddot{q}^{MDes} = \dot{q}^N + 2\Lambda_M (\dot{q}^N - \dot{q}^M) + \Lambda_M^2 (q^N - q^M), \quad (1)$$

with $\Lambda_M = 2 s^{-1}$ time-exponent. This model is more sophisticated than a *proportional controller* since from psychological point of view it can be expected that the user is apt to apply stronger feedback to compensate suddenly increasing error than it could be done by a simple P-type controller. (However, the surgeon is not expected to have the qualities of a PID-type controller that also contains integrated error in the feedback term.)

The arm assumes an angular momentum $I = 20 [kg \cdot m^2]$ on the basis of which a master control torque term $T_{ctrl}^M = I\ddot{q}^{MDes}$ is applied on the axle of the master arm. It is not assumed that the surgeon is in the possession of some quantitative model of the tissue to be cut. He/she only observes the presence of the cut material by feeling the “drag torque” generated by the matter. (The effects of this torque has to be compensated by the PD-type feedback only.) This drag torque is derived by the following assumption:

$$T_{drag}^M = -C_{id}\nu\dot{q}^M S^2\nu, \quad (2)$$

in which $v = \nu\dot{q}^M S$ describes the linear velocity of the cutting tool, $F_{drag} = -C_{id}v$ is the drag force exerted by the cut material with $C_{id} = 1.2 \times 10^4 [N \cdot s/m]$ linear drag coefficient, and $F_{drag}S\nu$ is the torque of this drag force scaled back to the rotary axle of the master arm. The actual angular acceleration of the master arm is $\ddot{q}^M = \frac{T_{ctrl}^M + T_{drag}^M}{I}$. The so generated $\{q^M, \dot{q}^M, \ddot{q}^M\}$ values describe the kinematically prescribed trajectory to be tracked by the slave system.

It is emphasized that any other “alternative” surgeon–master arm model should not yield hectic motion. This simple friction model is free of the phenomenon of *slipping*, therefore it is reasonable to use it as a reference model. In section III, the operation of the *slave arm* is described.

III. THE MODEL OF THE SLAVE SYSTEM

The plant is a DC-motor driven arm (via the application of gear reduction), and this arm is in dynamic interaction with a strongly nonlinear environment. The motor model and its appropriate parameters were taken from [31] as follows:

$$\begin{aligned} \ddot{q}^S &= \frac{Q_e + Q_{ext} - b\dot{q}^S - mgS \sin(\nu q^S)}{\Theta}, \\ \dot{Q}_e &= \frac{-RQ_e - K^2\dot{q}^S + KU}{L}, \end{aligned} \quad (3)$$

where $q^S [rad]$ denotes the rotational angle of the slave motor’s axle, $Q_e [N \cdot m]$ is the torque of electromagnetic origin exerted on the motor’s axle, $Q_{ext} [N \cdot m]$ is the torque of external origin acting on the motor’s axle, $\nu = 0.1$ is the gear reduction ratio, $R = 1 [\Omega]$ is the Ohmic resistance of the motor’s coil system, $L = 0.5 [H]$ is its inductivity, $\Theta = 0.01 [kg \cdot m^2]$ denotes the momentum of the rotary part

of the motor, $b = 0.1 \left[\frac{N \cdot m \cdot s}{rad} \right]$ describes the viscous friction of the motor's axle, $K = 0.01$ is the motor's torque coefficient, $g = 9.81 \left[\frac{m}{s^2} \right]$ denotes the gravitational acceleration, $S = 0.05 [m]$ is the length of the arm of the slave system (with neglected momentum), $m = 0.01 [kg]$ is the mass of the point-like burden at the end of the arm, and $U [V]$ denotes the motor control voltage.

The actual drag force of the cut material was modeled as follows:

$$F_w = -(C_w \sigma_2(\nu \dot{q}^S / D_w) - A_w \frac{(\nu \dot{q}^S / D_w)^3}{(1 + (\nu \dot{q}^S / B_w)^4)}) \quad (4)$$

in which $\sigma_2(x) \triangleq \frac{x}{1+|x|}$. This model has the qualitative properties to describe the stick-slip phenomenon. The torque of this force must be scaled by factor ν to describe its effect on the motor axle as $Q_{ext} = \nu S F_w$. In section IV, control issues of this model are discussed.

IV. THE RFPT-BASED DESIGN FOR ORDER REDUCTION

Assuming that $(\Lambda_S + \frac{d}{dt})^3 \int_{t_0}^t (q^M(\xi) - q^S(\xi)) d\xi \equiv 0$ (as an "ideal formula") is used to define the kinematically prescribed tracking error reduction $\Lambda_S > 0$, $q^M(t)$ is the master trajectory to be tracked, $q^S(t)$ is the actual one). It leads to the desired 2nd time-derivative that corresponds to a PID-type control as

$$\ddot{q}^{S^{Des}} \triangleq \ddot{q}^M + \Lambda_S^3 \int_{t_0}^t [q^M(\xi) - q^S(\xi)] d\xi + 3\Lambda_S^2 [q^M(t) - q^S(t)] + 3\Lambda_S [\dot{q}^M(t) - \dot{q}^S(t)], \quad (5)$$

resulting exponential error-relaxation for $\Lambda_S > 0$. In the given physical state of the system determined by the actual (q^S, \dot{q}^S) at a given external torque on the motor axle, Q_{ext} the first equation of the group (3) could be used to determine the *electromagnetic torque*, Q_e that would be necessary to guarantee the realization of $\ddot{q}^{S^{Des}}$. Unfortunately, the 2nd equation of (3) means that Q_e cannot be instantaneously set: by the application of an abrupt change in the control voltage U , only \dot{Q}_e can be forced to vary. Therefore in a precise control, (5) should be replaced by a policy that defines $\ddot{q}^{S^{Des}}$, and the time-derivative of the first equation in the group should be calculated in order to work with a 3rd order controller, to avoid the need to apply some order reduction techniques. While in the realm of the *Linear Time-Invariant* (LTI) systems that can be described in the frequency domain by fractional polynomial *Transfer Functions*, the Padé approximation theory [32] can widely be used for order reduction, even in the case of fractional order systems of long memory [33], in the case of nonlinear systems alternative approaches have to be chosen.

To avoid 3rd order control the RFPT-based order reduction can be formulated as follows: if \dot{q}^S would be constant the 2nd equation of (3) could describe a stable linear system that exponentially traces the abrupt jumps in U . If the electric components worked considerably faster than the mechanical ones, (3) could be used for designing abrupt changes in U to realize (5) in the control cycles. However, this is only an approximation. The role of the RFPT-based adaptive design

contributes to correct this preliminary design together with the effects of the modeling errors and unknown external disturbances. In this approach, $\ddot{q}^{S^{Des}}$ is computed from (5), but instead of the "exact model" in (4), the surgeon's reference model is used. By the use of the first equation of (3), Q_e^{Des} is calculated for $\ddot{q}^{S^{Des}}$. Assuming that $\dot{Q}_e \approx 0$ for a given constant \dot{q}^S , the stabilized value of the necessary U^{Des} is estimated from the 2nd equation as:

$$U^{Des} \triangleq \frac{R}{K} Q_e^{Des} + K \dot{q}^S. \quad (6)$$

In this manner a "response function" can be introduced that describes the "realized response of the system" \ddot{q}^S that actually is obtained for any input $\ddot{q}^{S^{Des}}$ that was calculated on kinematic basis and substituted into an available approximate model as $\ddot{q}^S = f(\ddot{q}^{S^{Des}})$ in which f also depends on q^S and \dot{q}^S that vary relatively slowly if \ddot{q}^S may have abrupt variation. The idea of adaptivity consists in finding a deformed value \ddot{q}_* for which $f(\ddot{q}_*) = \ddot{q}^{S^{Des}}$. We seek it by the use of an iterative sequence $\ddot{q}_n^{S^{Req}} \rightarrow \ddot{q}_*$ generated by a function as $\ddot{q}_{n+1}^{S^{Req}} \triangleq G(\ddot{q}_n^{S^{Req}}, \ddot{q}^{S^{Des}})$ in which the first element can be $\ddot{q}_0^{S^{Req}} = \ddot{q}^{S^{Des}}$.

$$\ddot{q}_{n+1}^{S^{Req}} = G(\ddot{q}_n^{S^{Req}}, \ddot{q}^{S^{Des}}) \triangleq \left(\ddot{q}_n^{S^{Req}} + K_c \right) \times \left\{ 1 + B_c \sigma \left(A_c \left[f(\ddot{q}_n^{S^{Req}}) - \ddot{q}_{n+1}^{S^{Des}} \right] \right) \right\} - K_c, \quad (7)$$

where A_c , B_c and K_c are adaptive control parameters, and the function $\sigma(x)$ is defined as follows:

$$\sigma(x) \triangleq \begin{cases} -1 & \text{if } x \leq -1, \\ x & \text{if } -1 < x < 1, \\ 1 & \text{if } x \geq 1. \end{cases} \quad (8)$$

Evidently, if $f(\ddot{q}_n^{S^{Req}}) = \ddot{q}_{n+1}^{S^{Des}}$, i.e., when the appropriate deformation is found, $\ddot{q}_{n+1}^{S^{Req}} = \ddot{q}_n^{S^{Req}} = \ddot{q}_*$, that is the solution of the control task is the fixed point of the mapping nearby the the zero argument of $\sigma(x)$ defined in (7). For convergence, this mapping must be made *contractive in the vicinity of this fixed point*. For a real differentiable function the simple estimation $|g(b) - g(a)| = \left| \int_a^b \frac{dg(x)}{dx} dx \right| \leq \int_a^b \left| \frac{dg(x)}{dx} \right| dx \leq K|b - a|$ holds if $\left| \frac{dg(x)}{dx} \right| \leq K$ therefore this fixed point will be contractive if its derivative in absolute value is smaller than 1 in its vicinity, i.e. $\left| 1 + \left(K_c + \ddot{q}^{S^{Req}} \right) B_c A_c \frac{df}{d\ddot{q}^{S^{Req}}} \Big|_{\ddot{q}^{S^{Req}} = \ddot{q}_*} \right| < 1$. To guarantee that normally $B_c = \pm 1$ depending on the sign of $\frac{df}{d\ddot{q}^{S^{Req}}} \Big|_{\ddot{q}_*}$, a very big $|K_c|$ and an appropriately small $A_c > 0$ value has to be chosen. (For the details on how to keep the system in the vicinity of this fixed point by complementary tuning of A_c we refer to [24], [25]). The behavior of this mapping at the trivial fixed point $-K_c$ and its global features that may lead to chaotic control signals were investigated in details in [34]. In this paper, this issue will not be addressed in details. In the followings, simulation results are presented.

V. SIMULATION RESULTS

The simulations were implemented using SCILAB 5.4.1 for LINUX and its graphical tool, called XCOS. Both are open access [35]. SCILAB offers various solvers (i.e., numerical integrators) for Ordinary Differential Equations. In the simulations, we used the *Livermore Solver for solving Ordinary Differential Equations* option (*LSodar*) that applies an automatic switching for stiff and non-stiff problems. It also uses variable step size and combines the (*Backward Differentiation Formula*) (BDF) and *Adams* integration methods. The stiffness detection is done by step size attempts in both cases. The “digital nature” of the controller was modeled by the application of *sample holders*, and in (7), the element called *continuous time delay* was used to utilize the past values in the iteration. Evidently, the necessary time-delay depends on the dynamics of the motion to be tracked and it also directly influences the available tracking precision.

To achieve useful results the allowable step-size was limited to 10^{-2} in the simulations by setting the solver. One of the advantages of the RFPT-based methods is that they can work with relatively small Λ_S values. In our case, $\Lambda_S = 1 \text{ s}^{-1}$ was applied in (5). We made simulations for various settings of the model-parameters in (4). Parameters $B_w = 0.2 [\frac{\text{s}}{\text{rad}}]$, and $D_w = 0.2 [\frac{\text{s}}{\text{rad}}]$ were kept constant. The adaptive control parameters were set as $B_c = -1$, $K_c = 10^8$ and $A_c = 10^{-9}$, and no tuning for A_c was necessary.

In the first set of the simulations drastic friction was assumed with the parameters $A_w = 30 \text{ [N]}$ and $C_w = 30 \text{ [N]}$. Simulations were performed for $\delta t = 10^{-4} \text{ s}$ and $\delta t = 10^{-3} \text{ s}$ cycle times. Figs. 1, 2 and 3 reveal that the master arm made precise tracking in spite of the great difference in the drag torques produced by the surgeon’s *reference model* and the actual tissue under cutting operation. The phenomenon of *slipping* is well indicated by the decreasing drag force with increasing velocity (red line in Fig. 4).

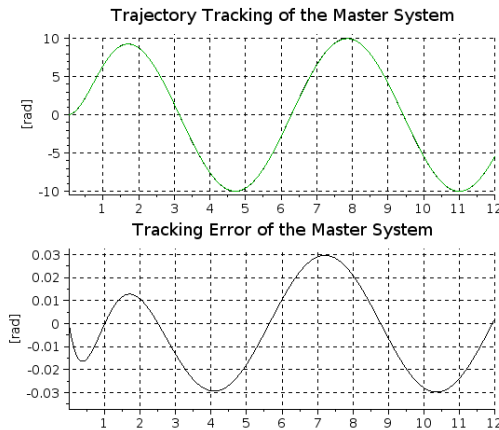


Fig. 1. The master motor trajectory tracking for strong friction at $\delta t = 10^{-4} \text{ s}$: nominal trajectory q^N (black line) and simulated q^M one (green line) vs. time [s] (upper chart) and the trajectory tracking error (lower chart).

Fig. 4 reveals that the actual drag-force has increasing and decreasing segments with increasing velocity while the simple

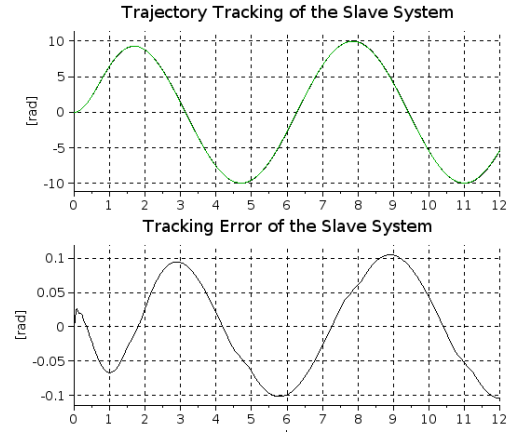


Fig. 2. The slave motor trajectory tracking for strong friction at $\delta t = 10^{-4} \text{ s}$: master trajectory q^M (black line) and simulated slave trajectory q^S one (green line) vs. time [s] (upper chart), and the trajectory tracking error (lower chart).

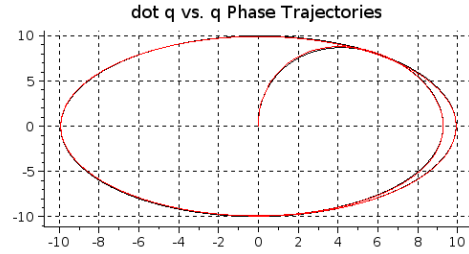


Fig. 3. Tracking of the master motor’s phase trajectory by the slave system (i.e. \dot{q} vs. q) at $\delta t = 10^{-4} \text{ s}$: master (black line) and simulated slave (red line) phase trajectories for the motor axle vs. time [s].

viscous model assumes only proportionality.

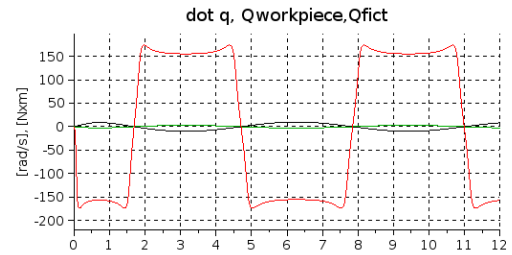


Fig. 4. The time-derivative the motor axle \dot{q}^S (black line), 1000 times the torque of the drag force by the environment estimated by the use of the reference model (green line), and the actual one (red line) vs. time [s] at $\delta t = 10^{-4} \text{ s}$.

To illustrate the RFPT-based adaptivity besides the 2nd time-derivative of the master trajectory \ddot{q}^M , the other relevant 2nd time-derivatives are described in Fig. 5. The master, the desired (i.e., the master corrected by the PID-type terms) and the *realized/simulated* \ddot{q}^S values are in each other’s close vicinity, while the adaptively deformed “required” value is significantly different.

The figures of the electromagnetic motor torque (Fig. 6) and the control voltage (Fig. 7) well exemplify the operation of the order reduction technique: in the graph of the control

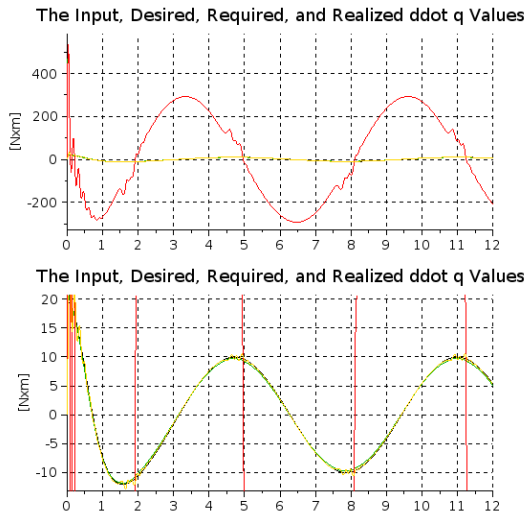


Fig. 5. The operation of the RFPT-based adaptivity in the case of the slave system at $\delta t = 10^{-4}$ s: \ddot{q}^M : black line, \ddot{q}^{SDes} : green line, \ddot{q}^{SReq} : red line, and \ddot{q}^S : other line vs. time [s].

voltage, fine transients can be observed when the adaptively deformed \ddot{q}^{SReq} suffers fast variation. Since these transients mainly concern the time-derivative of Q_e in the chart of the variation of Q_e , their effects is “hidden” by the integration.

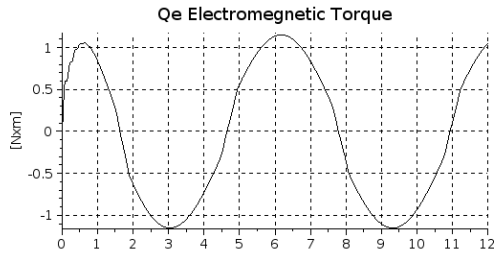


Fig. 6. The electromagnetic torque of the motor of the slave system vs. time [s] at $\delta t = 10^{-4}$ s.

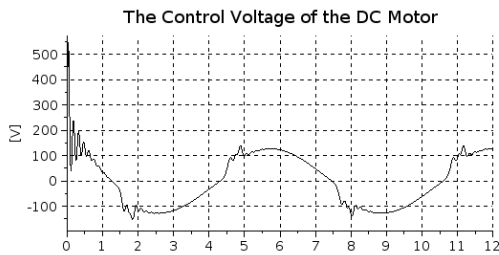


Fig. 7. The control voltage of the slave system vs. time [s] units at $\delta t = 10^{-4}$ s.

To investigate the effects of increasing the cycle time (that should be at maximum 1 ms for mechanical systems) simulations were made for at $\delta t = 10^{-3}$ s cycle-time. By comparing Figs. 2 and 8, it becomes evident that the tracking error increased but the main characteristics of the trajectory tracking remained the same. At gear ratio $\nu = 0.1$, the error

at the motor’s axle of the cutting tool is only about ± 0.1 rad at a motion of amplitude of 10rad that means 1 rad amplitude motion with ± 0.01 rad error at arm moving the cutting tool. Figs. 9 and 10 testify that the transient behavior is present at the fast changes of \ddot{q}^{SReq} , but its finer details disappeared. Also, the variation of Q_e became “less even” in this case. The tracking details seem to be more informative in the phase space (Fig. 11).

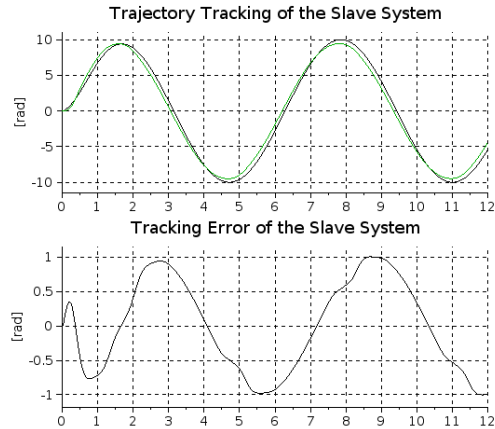


Fig. 8. The slave motor trajectory tracking for strong friction at $\delta t = 10^{-3}$ s: master trajectory q^M (black line) and simulated slave trajectory q^S one (green line) vs. time [s] (upper chart), and the trajectory tracking error (lower chart).

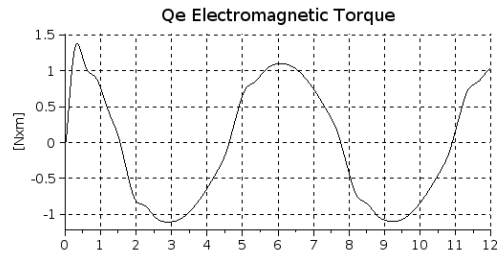


Fig. 9. The electromagnetic torque of the motor of the slave system vs. time [s] at $\delta t = 10^{-3}$ s.

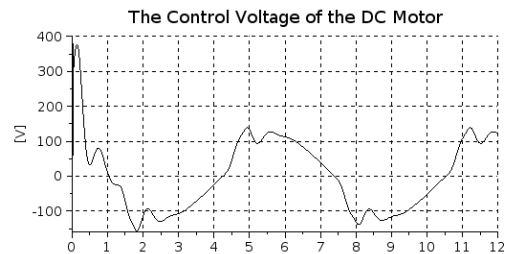


Fig. 10. The control voltage of the slave system vs. time [s] at $\delta t = 10^{-3}$ s.

VI. CONCLUSIONS

In this paper, a novel design methodology was suggested for the realization of a *Model Reference Adaptive Controller* for a master–slave system to be used for tissue cutting operations.

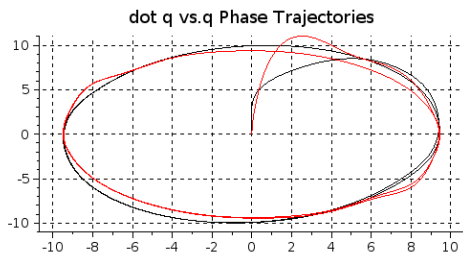


Fig. 11. Tracking of the master phase trajectory by the slave system (i.e. \dot{q} vs. q) at $\delta t = 10^{-3}$ s: master (black line) and simulated slave (red line) phase trajectories for the motor axle vs. time [s].

Its main advantage is simplicity; simultaneously realizing *adaptivity* and *order reduction* without using Lyapunov's complicated 2nd method. The master system consisted of the surgeon and a well behaving reference material model free of the inconvenient sticking effect. In our simulations, a simple model was used. It was not the aim of the paper to provide a particular, evidence-derived tool–tissue model, since those are under current investigations. These blocks can be replaced by different ones while the RFPT-based design can work in similar manner. In the future, we plan physical experiments to validate the simulation results.

ACKNOWLEDGMENT

The authors thankfully acknowledge the grant provided by the Project TAMOP-4.2.2.A-11/1/KONV-2012-0012: *Basic research for the development of hybrid and electric vehicles*. The Project is supported by the Hungarian Government and co-financed by the European Social Fund. Our work has been partially supported by the *Hungarian Scientific Research Fund OTKA K-106392*. T. Haidegger and L. Kovács are Bolyai Fellows of the Hungarian Academy of Sciences.

REFERENCES

- [1] A. Hibi and T. Ichikawa. Mathematical model of the torque characteristics for hydraulic motors. *Bull. JSME*, 20(143):616–621, 1977.
- [2] D.P. Hess and A. Soom. Friction at a lubricated line contact operating at oscillating sliding velocities. *ASME J. Tribology*, 112(1):147–152, 1990.
- [3] B. Armstrong-Helouvy. Stick slip and control in low-speed motion. *IEEE Trans. on Automatic Control*, 38(10):1483–1496, 1990.
- [4] B. Armstrong-Helouvy. *Control of machines with friction*. Kluwer Academic Publishers, 1991.
- [5] B. Armstrong-Helouvy, P. Dupont, and C. Canudas de Wit. A survey of models, analysis tools and compensation methods for the control of machines with friction. *Automatica*, 30(7):1083–1138, 1994.
- [6] T.D. Gillespie. *Fundamentals of Vehicle Dynamics (1st edition)*. SAE International, 1992.
- [7] H.B. Pacejka and E. Bakker. The magic formula tyre model. *Vehicle System Dynamics*, 21:1–18, 1993.
- [8] J.J.M. van Oosten and E. Bakker. Determination of magic tyre model parameters. *Vehicle System Dynamics*, 21:19–29, 1993.
- [9] L. Lidner. Experience with the magic formula tyre model. *Vehicle System Dynamics*, 21:30–46, 1993.
- [10] C. Canudas de Wit, H. Olsson, K.J. Åström, and P. Linschinsky. A new model for control of systems with friction. *IEEE Trans. Automatic Control*, 40(3):419–425, 1995.
- [11] J. Swevers, J. F. Al-Bencer, C.G. Ganseman, and T. Prajogo. An integrated friction model structure with improved presliding behavior for accurate friction compensation. *IEEE Trans. Automatic Control*, 45(4):675–686, 2000.
- [12] P. Dupont, V. Hayward, B. Armstrong, and F. Altpeter. Single state elastoplastic friction models. *IEEE Trans. Automatic Control*, 47(5):787–792, 2002.
- [13] G. Rill. *Simulation von Kraftfahrzeugen*. Vieweg+Teubner Verlag, 1994.
- [14] V. Kálmán and L. Vajta. Slip based center of gravity estimation for transport robots. In: *Proc. of Factory Automation, University of Pannonia, Veszprém*, pages 50–55, 2012.
- [15] L. Márton and B. Lantos. Identification and model-based compensation of stribbeck friction. *Acta Polytechnica Hungarica*, 3(3):45–58, 2006.
- [16] A.M. Lyapunov. *A general task about the stability of motion. (in Russian)*. PhD Thesis, University of Kazan, 1892.
- [17] A.M. Lyapunov. *Stability of motion*. Academic Press, New-York and London, 1966.
- [18] R. Isermann, K.H. Lachmann, and D. Matko. *Adaptive Control Systems*. Prentice-Hall, New York DC, USA, 1992.
- [19] Jean-Jacques E. Slotine and W. Li. *Applied Nonlinear Control*. Prentice Hall International, Inc., Englewood Cliffs, New Jersey, 1991.
- [20] R.M. Murray, Z. Li, and S.S. Sastry. *A mathematical introduction to robotic manipulation*. CRC Press, New York, 1994.
- [21] J.K. Tar, J.F. Bitó, L. Náđai, and J.A. Tenreiro Machado. Robust Fixed Point Transformations in adaptive control using local basin of attraction. *Acta Polytechnica Hungarica*, 6(1):21–37, 2009.
- [22] S. Banach. Sur les opérations dans les ensembles abstraits et leur application aux équations intégrales (About the Operations in the Abstract Sets and Their Application to Integral Equations). *Fund. Math.*, 3:133–181, 1922.
- [23] J.K. Tar. Towards replacing Lyapunov's "direct" method in adaptive control of nonlinear systems (invited plenary lecture). In: *Proc. of the Mathematical Methods in Engineering International Symposium (MME 2010), Coimbra, Portugal*, 2010.
- [24] J.K. Tar, L. Náđai, I.J. Rudas, and T.A. Várkonyi. RFPT-based adaptive control stabilized by fuzzy parameter tuning. *9th European Workshop on Advanced Control and Diagnosis (ACD 2011), Budapest, Hungary*, pages 63–68, 2011.
- [25] K. Kósi, J.K. Tar, and I.J. Rudas. Improvement of the stability of RFPT-based adaptive controllers by observing "precursor oscillations". *A Proc. of the 9th IEEE International Conference on Computational Cybernetics, 8-10 July 2013, Tihany, Hungary*, pages 267–272, 2013.
- [26] C.C. Nguyen, S.S. Antrazi, Zhen-Lei Zhou, and C.E. Campbell Jr. Adaptive control of a stewart platform-based manipulator. *J. of Robotic Systems*, 10(5):657–687, 1993.
- [27] R. Kamnik, D. Matko, and T. Bajd. Application of model reference adaptive control to industrial robot impedance control. *Journal of Intelligent and Robotic Systems*, 22:153–163, 1998.
- [28] J. Somló, B. Lantos, and P.T. Cát. *Advanced Robot Control*. Akadémiai Kiadó, Budapest, 2002.
- [29] K. Hosseini-Sunay, H. Momeni, and F. Janabi-Sharifi. Model reference adaptive control design for a teleoperation system with output prediction. *J. Intell. Robot Syst.*, pages 1–21, 2010.
- [30] J.K. Tar, J.F. Bitó, I.J. Rudas, and K. Eredics. Comparative analysis of a traditional and a novel approach to Model Reference Adaptive Control. *11th International Symposium of Hungarian Researchers on Computational Intelligence and Informatics, Budapest, Hungary*, pages 93–98, 2010.
- [31] <http://ctms.engin.umich.edu/CTMS/index.php?example=MotorSpeed§ion=SystemModeling>. Last accessed: July 1, 2014.
- [32] H. Padé. *Sur la représentation approchée d'une fonction par des fractions rationnelles (Thesis)*. Ann. École Normale. (3)9, 1892, pp. 1–93 suppl., 1892.
- [33] R.S. Barbosa and J.A. Tenreiro Machado. Implementation of discrete-time fractional-order controllers based on LS approximations. *Acta Polytechnica Hungarica*, 3(4):5–22, 2006.
- [34] K. Kósi, Sz. Hajdu, J.F. Bitó, and J.K. Tar. Chaos formation and reduction in Robust Fixed Point Transformations based adaptive control. *4th IEEE International Conference on Nonlinear Science and Complexity (NSC 2012), Budapest, Hungary*, pages 211–216, 2012.
- [35] <http://www.scilab.org>. Last accessed: July 1, 2014.